Provided for non-commercial research and education use.
Not for reproduction, distribution or commercial use.

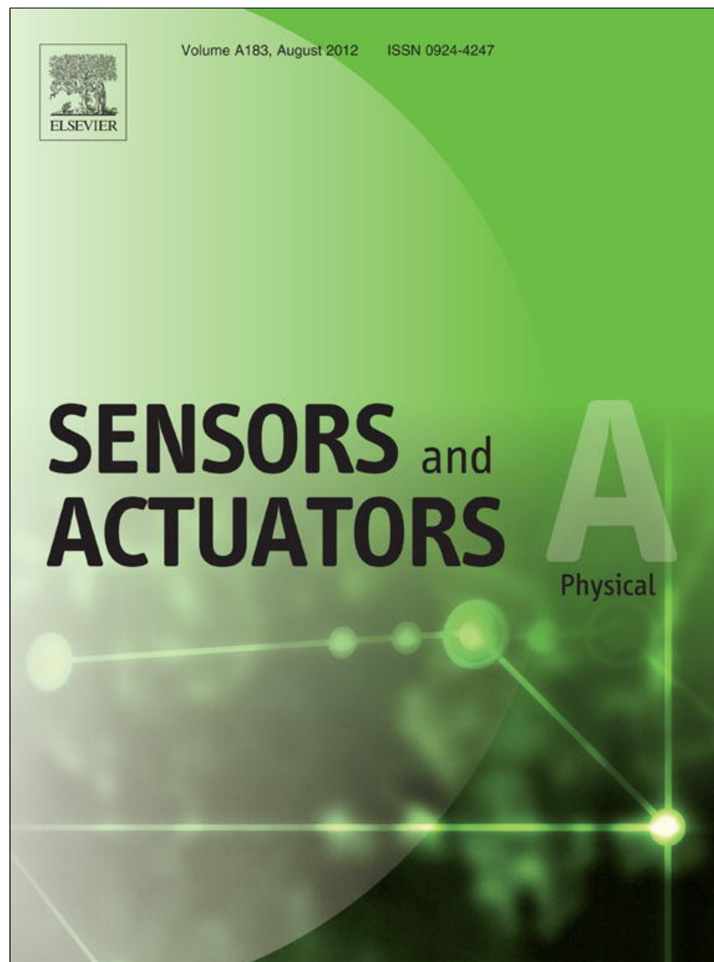

This article appeared in a journal published by Elsevier. The attached copy is furnished to the author for internal non-commercial research and education use, including for instruction at the authors institution and sharing with colleagues.

Other uses, including reproduction and distribution, or selling or licensing copies, or posting to personal, institutional or third party websites are prohibited.

In most cases authors are permitted to post their version of the article (e.g. in Word or Tex form) to their personal website or institutional repository. Authors requiring further information regarding Elsevier's archiving and manuscript policies are encouraged to visit:

http://www.elsevier.com/copyright

Author's personal copy

Sensors and Actuators A 183 (2012) 95–100

Contents lists available at SciVerse ScienceDirect

Sensors and Actuators A: Physical

journal homepage: www.elsevier.com/locate/sna

Design and characterization of a fully compliant out-of-plane thermal actuator

K. Ogando, N. La Forgia [1], J.J. Zárate, H. Pastoriza *

Comisión Nacional de Energía Atómica, Laboratorio de Bajas Temperaturas, Centro Atómico Bariloche & Instituto Balseiro, (8400) S.C. de Bariloche, Argentina

ARTICLE INFO

Article history:
Received 14 September 2011
Received in revised form 10 May 2012
Accepted 15 May 2012
Available online 24 May 2012

Keywords:
Surface micro-machining
Thermal actuators

ABSTRACT

This paper presents the design and characterization of an out-of-plane thermal actuator. The design optimizes the vertical displacement by concentrating elastic deformations in localized hinges allowing a full thermal expansion of the actuator arms. Heating is provided by Joule dissipation in the actuator itself. A testing device was fabricated using the Memscap PolyMUMPs process. Characterization of the sensor was performed by white light optical profilometry for varying electric biasing and different atmospheres. The presented design has the advantage that the moving direction of the actuator can be determined by the relative location of the hinges.

© 2012 Elsevier B.V. All rights reserved.

1. Introduction

Many applications of micro-systems require actuators that displace out-of-plane from the substrate. Adaptive optics [1] and steering mirrors [2,3] being some examples. With conventional surface micro-machining processes this motion is hard to realize in a fully compliant design due to the limitations in the fabrication technology. Several transducing mechanisms to produce motions from electrical signals in microsystems had been proposed and developed [4]. Within the huge variety of actuators electro-thermal ones base its mechanism in the displacement caused by the thermal expansion of some of the actuator components induced by Joule heating [5]. This type of actuators has the advantage of requiring low voltage drive with high stroke and force.

For out-of-plane actuation two different types of transducers are usually found in the literature: those where displacement is produced from the dissimilar thermal expansion of the materials in multi-layers also called bimorph effect [3], and those where the out of plane motion arises from the buckling induced by thermal expansion of a double clamped beam [6,7]. Both approaches have some advantages and drawbacks. In the bimorph effect case large displacements can be obtained but shear forces at the interfaces induce de-lamination after a long term operation [8]. On the other hand, buckling based actuators benefit from the possibility of being fabricated from a single layer structure. However in these actuators the direction of displacement and efficiency are strongly dependent on residual stress and topology [9]. Other drawbacks are present in buckling based thermal actuators. One is the low ratio between displacement to dissipated power due to elastic energy stored in the deformed beam. Another is existence of a power threshold that should be reached in order to superate the buckling instability. This difficults their operation in applications requiring small and accurate strokes [10].

Another issue that has to be taken into account on the design stage or during the fabrication is the necessity of forcing a break in symmetry to condition the displacement direction. This is usually done by taking advantage of residual stress from the fabrication process [9] or with the design of *chevron*-like structures [11,12]. Some recent works present designs where broken symmetry is achieved by double campled step-beam designs [13–15]. In this examples the entire bar is subjected to deformation which does not minimize the elastic energy cost due distortion.

In the present paper the proof of concept of a new compliant electro-thermal actuator that combine flexural hinges with fully expanded beams is presented. The design addresses those limitations mentioned before following the design rules of the multiuser commercial process PolyMUMPs of Memscaps Inc. [16].

2. Out-of-plane actuator design

2.1. Concept

The design is based on the principle of a double-clamped beam subject to thermal expansion. In order to optimize the out-of-plane displacement four weakened regions were inserted along the beam. These regions act as a compliant flexural hinges concentrating most of the elastic deformations. In this way the main portion of the beam can fully expand by thermal expansion by minimizing the elastic energy accumulated by bending or buckling. Many strategies can be followed to create these hinges. The simplest one is through

* Corresponding author. Tel.: +54 2944 445113; fax: +54 2944 445299.
E-mail address: hernan@cab.cnea.gov.ar (H. Pastoriza).
[1] Present address: Norwegian University of Science and Technology, N7030 Trondheim, Norway..

0924-4247/$ – see front matter © 2012 Elsevier B.V. All rights reserved.
http://dx.doi.org/10.1016/j.sna.2012.05.028

Author's personal copy

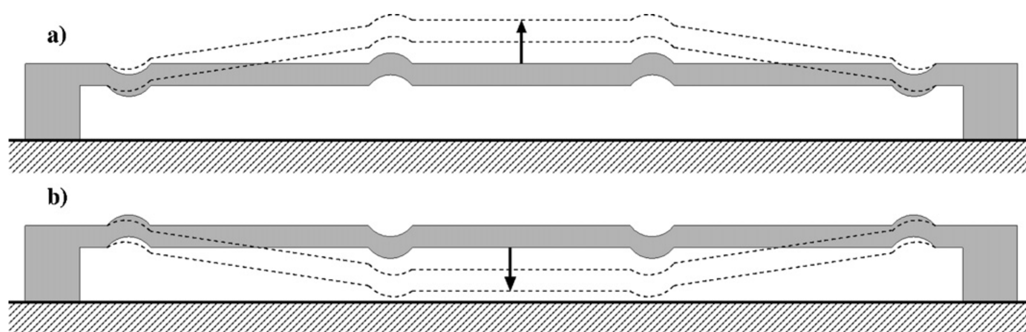

Fig. 1. Conceptual sketch of the proposed design. (a) Hinges placement to obtain an upward displacement upon thermal expansion (dotted lines). (b) Configuration to obtain a downward displacement.

the design of a lateral section reduction on the beam [17]. This approach has the advantage on the simplicity for the fabrication but a lateral reduction on the beam section does not contribute on the determination of a preferred vertical displacement direction. Another possible approach is a section reduction on the beam height, however this it is difficult to implement within the PolyMUMPs technology, due to the fixed polysilicon thickness in this process. In our case we have constructed the hinges using the *conformity* of the polysilicon deposition. The deposition of a polysilicon bar crossing a small oxide hole will generates a *V*-like dip in the bar that will concentrates elastic deformations on actuation. With this structure we can construct an upturning hinge. Similarly, the construction of a down-turning hinge can be realized by depositing the polysilicon bar on top of a oxide bump generating a Ω-like structure. The relative placement of these hinges along each arm of the actuator will determine the displacement direction of the membrane. Placing two upturn hinges close to each of the clamped extremes of the beam and downturn ones close to the middle of the beam creates an actuator that would move up on heating as is sketched in Fig. 1a. On the other way around, locating upturn hinges in the middle and the downturn ones next to the fixation points would induce that the structure moves towards the substrate on heating (see Fig. 1b). It is important to note that in our design the out-of-plane movement is produced by the bending of the hinges and not by arm's buckling. This results in a linear displacement regime for low dissipated power without any threshold as in buckling based actuators.

3. Fabrication process

The multi-user MEMS process (PolyMUMPs®) from MEMSCAP Inc. [16] was chosen for the fabrication of the devices. This process offers two structural layers of polysilicon (Poly1 and Poly2) and two sacrificial layers of phosphosilicate glass (Ox1 and Ox2). Besides the full patterning of these layers and the underlying contact layer also of polysilicon (Poly0) a dimple layer is provided that allows the partial etching of the first oxide. The substrate is electrically isolated from all polysilicon layers by a nitride layer.

Different combinations for structural layer and hinge formation were explored within this technology obtaining similar performances. Using Poly2 layer as the actuator layer, upturn hinges were defined by a hole in the Ox2 layer with (model A5) or without superposition with a dimple (models A3 and A6), or just a dimple (model A4). Downturn hinges were created by the bump induced by a small structure in the Poly0 layer. Similar device can be constructed using the Poly1 layer or even a double stack (Poly1 and Poly2) polysilicon. Fig. 2 presents the plan view and cross section of different models of these actuators.

4. Experimental characterization

In order to demonstrate the proposed concept different models of the actuators were fabricated and characterized. All actuators reported herein were designed using Poly2 as structural layer with 50 μm long, 2 μm wide arms, and a 50 μm × 50 μm central membrane. Several combination of hinges as detailed in Table 1 were essayed. Fig. 3 shows a SEM image of one device (A5) detailing the resultant geometry of the hinges.

The devices were tested and characterized on applying a dc electrical current through the whole device. Current and voltage were simultaneously measured in order to estimate the dissipated power.

The measurement of the vertical displacement was carried out by white light interferometry using a Veeco NT-1100 optical profilometer operating on the phase shift (PSI) mode when accuracy was required, and on VSI mode for large vertical range measurements. The on-plane resolution of the equipment (2 μm/pixel) is not good enough to resolve the arms of the device. Only the central platform can be diffraction-free imaged. The vertical accuracy of the setup is a few Ångstrom, with repeatability of 0.5 nm.

The response of the devices as a function of the applied power is shown in Fig. 4. It can be deducted from these data that the most efficient upturn hinge is that fabricated using both etching process (dimple and Poly1–Poly2 via) and the worst that realized when only the dimple layer was used. This indicates that there is an correlation between deepness of the etching hole with the actuator's efficiency. (dimple: 0.75 μm; Poly1–Poly2 via 1.1 μm [18]). Another observation from these data is the lower efficiency obtained using a downturn hinge of 4 μm in length in comparison to the 3 μm long one. This is consistent with a detailed calculation of the hinge efficiency to be submitted elsewhere [19].

The efficiency is small on air environment and improves significantly by pumping the surrounding gas, becoming better as the pressure decreases (see inset). This behavior is expected in thermal actuators as the principal source of heat losses is the conduction through the air.

At low excitations (<5 mW) the displacement is linear with the dissipated power. On increasing power the deflection becomes

Table 1
Detail of the different combination of methods to fabricate the conformal hinges.

Model	Downturn hinge	Upturn hinges
A3	3 μm Poly0 bump	3 μm Poly1–Poly2 via
A4	3 μm Poly0 bump	3 μm dimple
A5	3 μm Poly0 bump	3 μm dimple and Poly1–Poly2 via
A6	4 μm Poly0 bump	3 μm Poly1–Poly2 via

Author's personal copy

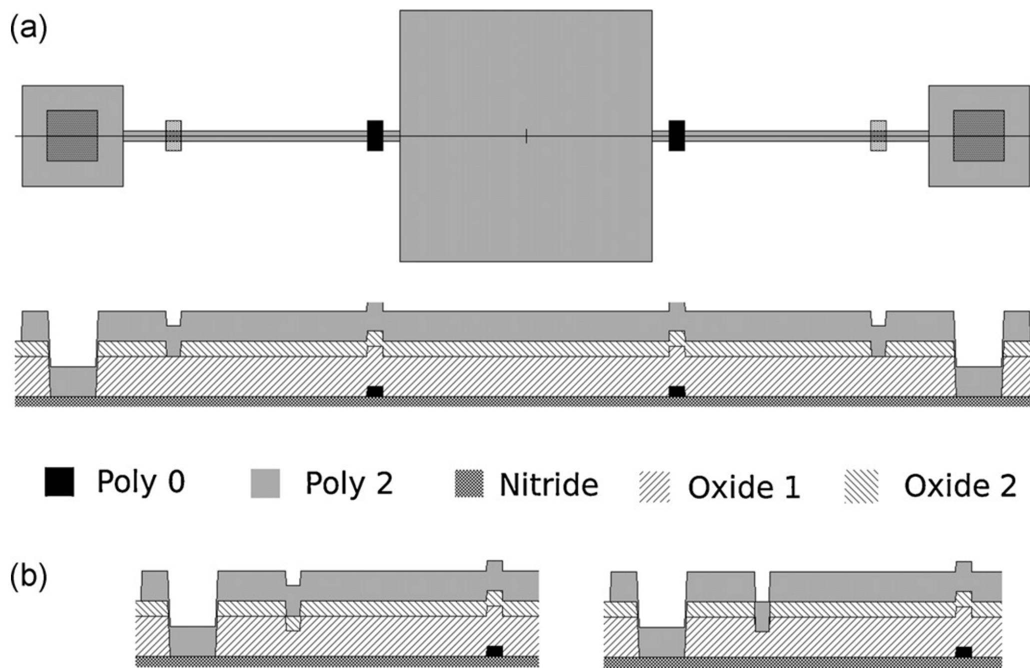

Fig. 2. (a) Schematic plan and cross view of one designed actuator (A3) within PolyMUMPs process. (b) Detail cross view of model A5. (c) Detail cross view of model A4 (see Table 1). The vertical scale in all cross sections is amplified five times. The apparent disconnection between Poly2 layer and Poly0 at anchors is an drawing artifact of this amplification. Fulfilling the Polymups design rules guarantees a correct anchoring because conformity of the polysilicon deposition.

nonlinear with a higher increase rate. The range of actuation for voltages up to 3V is of about 150 nm, with a power consumption of only 2 mW. The inset of Fig. 4 shows the response on a larger scale, highlighting that the actuator can be displaced several tens of nm even in air, by increasing the strength of excitation. The actuator responsiveness is on the lineal range of about 50 nm/mW for pressures below 100 mTorr.

5. Finite elements results

To complete the device behavior description we performed finite elements simulations specially to get insight on the deformation modes of the arms.

To run the numerical simulations, we used the commercial software CoventorWare® [20], which was specifically developed to be

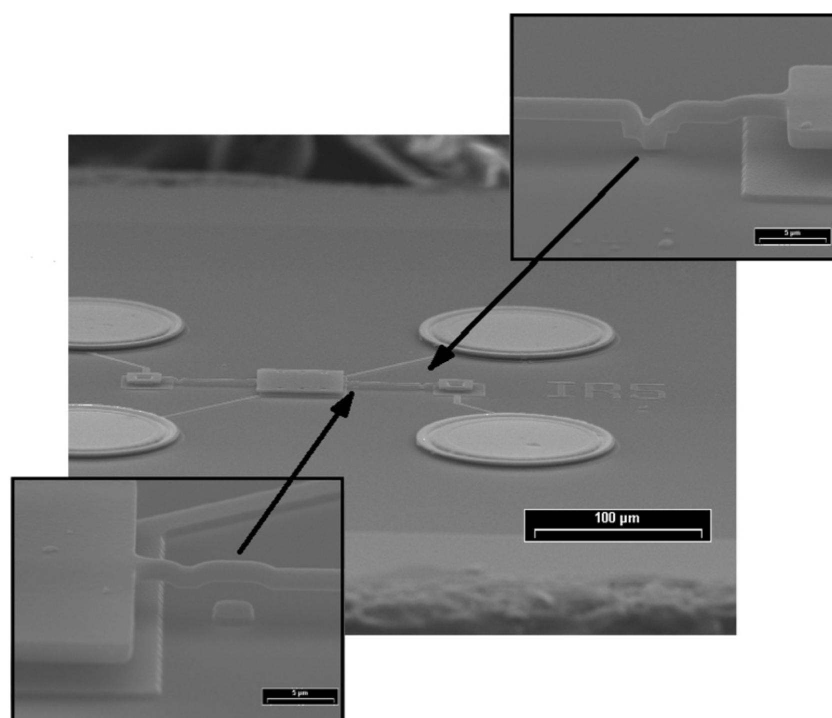

Fig. 3. Scanning electron microscope image tilted 45° of the actuator. Zoomed images of the hinges are depicted in the inserts.

Author's personal copy

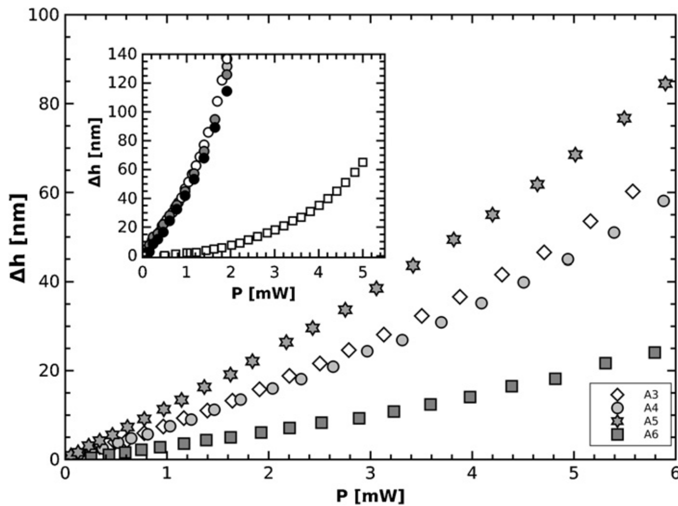

Fig. 4. Vertical displacements measured by optical profilometry as a function of the dissipated power for different actuator models. Inset: Vertical displacement of actuator A4 for different surrounding air pressures. Open squares: 1 bar, black circles: 10^{-3} mbar, grayed circles: 10^{-4} mbar, and open circles: 10^{-5} mbar.

used on microsystems simulations and include a module with the PolyMUMPs process variables and materials properties preloaded.

The processing of the data was performed sequentially using the output of an electro-thermal simulation to feed the input of an thermo-mechanical simulation. The electro-thermal simulation calculates the temperature profile due to Joule heating ignoring the deformations induced by thermal dilatation. After that a thermo-mechanical simulation uses the Joule heating results to calculate the temperature profile and the consequent mechanical deformation. This approach is only valid if deformations are small compared to the device size.

The solid model was created from the layout submitted to the Memscap foundry. It has not been taken into account in the simulation the silicon substrate, the contacts and polysilicon tracks. The mesh was generated through an extruded bricks algorithm which generate vertical prisms as mesh elements. To improve the effectiveness of the mesh the nominal size of the elements was set relatively wide but with a restriction of at least two elements by edge. In this way the complexity of the mesh only grows where was required by the geometry of the device.

5.1. Electro-thermal model

The first step of the simulation was aimed to calculate the Joule heating ignoring the deformations of the structure caused by thermal expansion. In the next paragraphs the details of the model will be developed.

The substrate was considered as a huge thermal mass at room temperature. In the simulation this fix a boundary condition of constant temperature at the bottom surface of the SiN_x layer.

The device is heated by Joule effect as the electrical current flows through the arms of the actuator due to the finite electrical resistance of the polysilicon structural material. For the electrical–thermal simulations, a difference in the electric potential were introduced as a boundary condition between the contacts pads of the actuator.

It is well known [21,22] that for these types of devices close to room temperature most of the heat losses occur by conduction. In particular the main contribution for microsystems of these sizes is the conduction through the surrounding air. Therefore it becomes indispensable the inclusion of this heat transport mechanism in the model in order to obtain reliable results.

To model the air mass around the device we included in the simulation an homogeneous solid surrounding the device with the electrical and thermal properties of the real air and with zero Young modulus. Because the limitations of the software heating the system results that the solid air expands differently than the device and the thermal contact is lost between the device and the air. To overcome this effect we divided the simulation in two consecutive parts: first we calculate the heating without taking into account deformations and therefore maintaining the thermal contact between the air and the device: In a second step we estimate the deformations and the mechanical behavior where the air has no effect due to the imposed softness.

In summary the boundary conditions were the constant temperature of the substrate and the electrical potential difference between the anchors of the actuator arms. The initial condition was an homogeneous room temperature on all the elements of the simulation.

5.2. Thermo-mechanical model

For the thermo-mechanical simulation the Joule heating profile calculated in the electro-thermal simulation was used as input and from there calculate the quasi-static deformation of the device. The boundary conditions for this stage consisted a fixed position for the anchors and substrate and the constant temperature of the substrate. The initial condition was setting room temperature for all elements in the simulation.

It is well known that is important to take into account the variations of the thermal and electrical properties of material with temperature in numerical calculations of silicon devices. In the present study case the validity of the numerical results were tested by running some simulations with variable physical parameters using the data compiled by Atre [22] for PolyMUMPs based devices.

5.3. Results

Fig. 5 shows the mechanical effects of the heating on the actuator. At the bottom of the figure we present the shape of the simulated actuator before heating. The top figure shows the shape of the actuator upon heating. The deformations are exaggerated 25 times in the z direction to highlight the qualitative characteristics. It can be seen that the upward displacement of the membrane occur mainly with deformations at the ends of the arms.

In Fig. 6a we present the vertical displacement along the device when it is actuated in vacuum with a applied power of 1.92 mW. Fig. 6b shows a cut of the von Misses stress calculated from the same simulation indicating its accumulation near the hinges. In parts (c) and (d) of Fig. 6 the temperature profile along the device when simulated in vacuum for an applied power of 1.92 mW and in air for an applied power of 10.5 mW respectively. It is evident the difference between both cases, in vacuum the maximum temperature is at the platform with a gradient in the arms up to room temperature in the bottom end. When the atmosphere is present the conduction through the air cools the platform generating a different distribution of temperature. In this case the maximum temperature is along the arms and the platform is at an intermediate temperature.

Quantitatively the differences are also important. The power dissipated by the device in the air simulation is ten times larger than that dissipated in vacuum. However the maximum temperature is much higher in the last case. This is directly related with losses through the air.

Finally Fig. 7 shows the comparison between the displacement measured and the calculated for air and vacuum. In the vacuum case the results are qualitatively similar. In the air case the real device is significantly more efficient than what is predicted by the

Author's personal copy

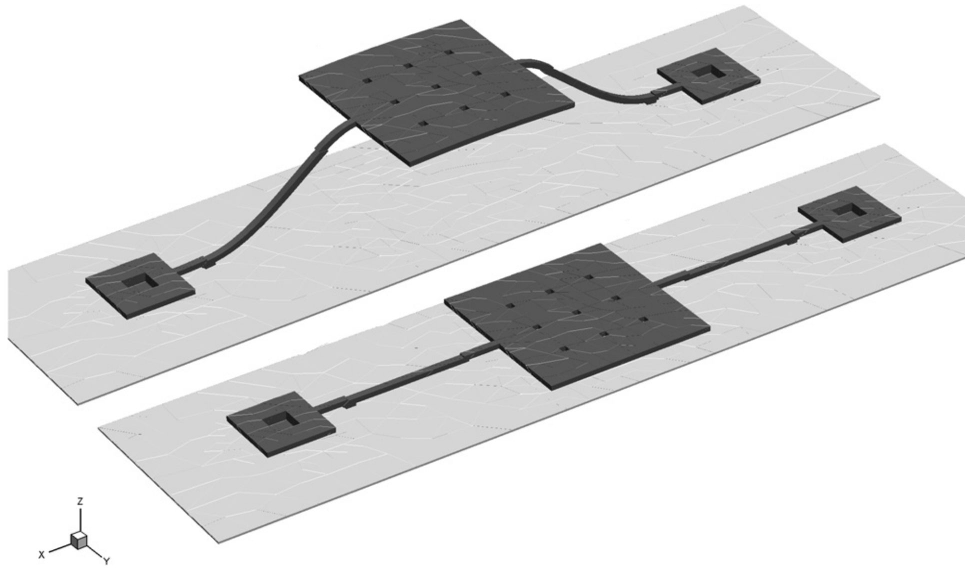

Fig. 5. Image reconstructed from finite elements calculation for the mechanical deformation of the actuator. The lower part shows the shape of the actuator before heating. Upper part shows the actuator displacement with the vertical scale augmented 25 times.

simulations. Evidently the model approach for the surrounding air over estimates the heat conduction. The stars correspond to the results of the simulations where the variation of the physical properties of the materials with temperature was taken into account. It

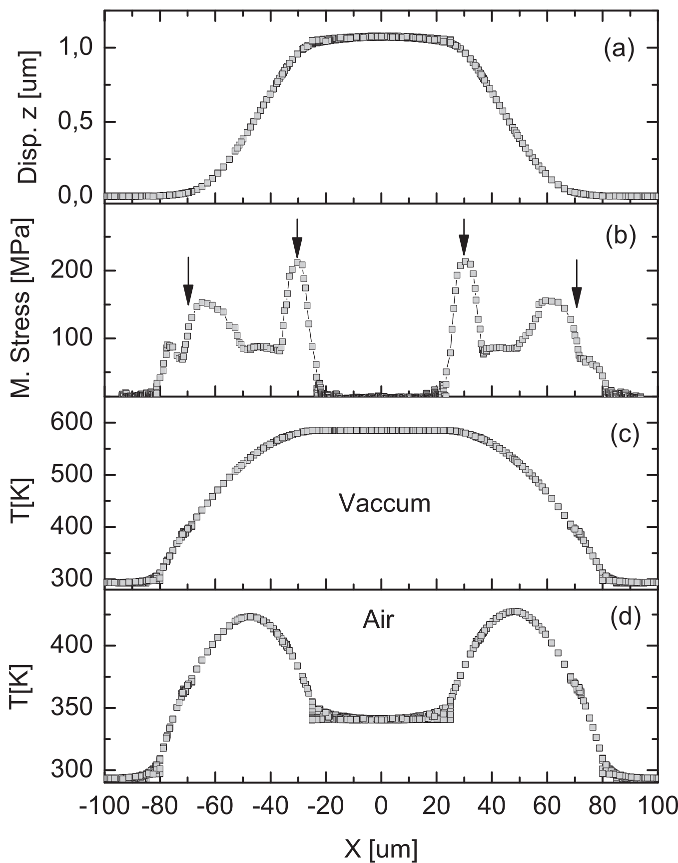

Fig. 6. (a) Vertical displacement along the device calculated from finite elements simulation when it is actuated in vacuum with an applied power of 1.92 mW. (b) von Misses stress along the device from simulation in the same conditions. Arrows indicate the position of the hinges. (c) Temperature profile along the device simulated in vacuum for the same applied power. (d) Temperature profile along the device when an air atmosphere was included in the simulation for an applied power of 10.5 mW.

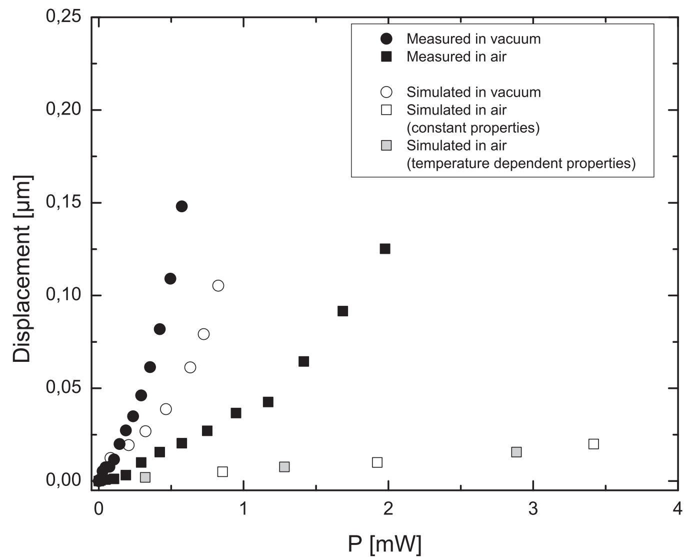

Fig. 7. Comparison of the measured (filled symbols) and simulated (open and grayed symbols) response. Both results are qualitative similar in vacuum (circles) but big discrepancies are found in air (squares) indicating that the numerical model is over estimating the heat losses.

can seen that this factor is not significant under our experimental conditions.

6. Conclusions

We have presented a simple thermal actuator design that can be realized following the Memscaps PolyMUMPs commercial process. Using the conformity of the polysilicon deposition process we were able to design upturn and downturn compliant hinges along the actuator arms. These hinges concentrate most of the elastic deformation energy allowing that most of the actuator arms expands free of tension by thermal Joule heating. As expected for thermal microsystems the response and efficiency of the device is dependent on the atmospheric conditions due the significant heat conduction through the surrounding air. By changing the fabrication method more efficient hinges could be realized.

Author's personal copy

Acknowledgements

This work was partially supported by INVAP S.E. and ANPCyT through grant PAE 2006 37063 – PID 137.

References

[1] D. Dagel, W. Cowan, O. Spahn, G. Grossetete, A. Grine, M. Shaw, P. Resnick, J.B. Jokiel, Large-stroke mems deformable mirrors for adaptive optics, Journal of Microelectromechanical Systems 15 (3) (2006) 572–583, http://dx.doi.org/10.1109/JMEMS.2006.876794.

[2] S. Leopold, D. Paetz, F. Knoebber, T. Polster, O. Ambacher, S. Sinzinger, M. Hoffmann, Tunable refractive beam steering using aluminum nitride thermal actuators, Proceedings of SPIE 7931 (2011) 79310B, http://dx.doi.org/10.1117/12.874826.

[3] S. Schweizer, S. Calmes, M. Laudon, P. Renaud, Thermally actuated optical microscanner with large angle and low consumption, Sensors and Actuators A: Physical 76 (13) (1999) 470–477, http://dx.doi.org/10.1016/S0924-4247(99)00012-6.

[4] D.J. Bell, T.J. Lu, N.A. Fleck, S.M. Spearing, Mems actuators and sensors: observations on their performance and selection for purpose, Journal of Micromechanics and Microengineering 15 (7) (2005) S153, http://dx.doi.org/10.1088/0960-1317/15/7/022.

[5] J.H. Comtois, V.M. Bright, Applications for surface-micromachined polysilicon thermal actuators and arrays, Sensors and Actuators A: Physical 58 (1) (1997) 19–25, http://dx.doi.org/10.1016/S0924-4247(97)80220-8.

[6] L. Sainiemi, K. Grigoras, I. Kassamakov, K. Hanhijrvi, J. Aaltonen, J. Fan, V. Saarela, E. Hggstrm, S. Franssila, Fabrication of thermal microbridge actuators and characterization of their electrical and mechanical responses, Sensors and Actuators A: Physical 149 (2) (2009) 305–314, http://dx.doi.org/10.1016/j.sna.2008.11.031.

[7] L. Lin, S.-H. Lin, Vertically driven microactuators by electrothermal buckling effects, Sensors and Actuators A: Physical 71 (12) (1998) 35–39, http://dx.doi.org/10.1016/S0924-4247(98)00167-8.

[8] E. Blank, J. Michler, Current issues in mechanics of layer systems for sensors and actuators, in: B. Kramer (Ed.), in: Advances in Solid State Physics 38, Advances in Solid State Physics, vol. 38, Springer Berlin, Heidelberg, 1999, pp. 593–605, http://dx.doi.org/10.1007/BFb0107646.

[9] T. Seki, M. Sakata, T. Nakajima, M. Matsumoto, Thermal buckling actuator for micro relays, in: International Conference on Solid State Sensors and Actuators, TRANSDUCERS '97, vol. 2, Chicago, 1997, pp. 1153–1156, http://dx.doi.org/10.1109/SENSOR.1997.635409.

[10] M. Chiao, L. Lin, Self-buckling of micromachined beams under resistive heating, Journal of Microelectromechanical Systems 9 (1) (2000) 146–151, http://dx.doi.org/10.1109/84.825789.

[11] M. Sinclair, A high force low area mems thermal actuator, in: The Seventh Intersociety Conference on Thermal and Thermomechanical Phenomena in Electronic Systems, ITHERM 2000, vol. 1, 2000, p. 132, doi:10.1109/ITHERM.2000.866818.

[12] J. Varona, M. Tecpoyotl-Torres, A.A. Hamoui, Design of mems vertical-horizontal chevron thermal actuators, Sensors and Actuators A: Physical 153 (1) (2009) 127–130, http://dx.doi.org/10.1016/j.sna.2009.04.027.

[13] W.-C. Chen, C.-C. Chu, J. Hsieh, W. Fang, A reliable single-layer out-of-plane micromachined thermal actuator, Sensors and Actuators A: Physical 103 (1–2) (2003) 48–58, http://dx.doi.org/10.1016/S0924-4247(02)00315-1.

[14] D. Girbau, M. Llamas, J. Casals-Terre, X. Simo-Selvas, L. Pradell, A. Lazaro, A low-power-consumption out-of-plane electrothermal actuator, Journal of Microelectromechanical Systems 16 (3) (2007) 719–727, http://dx.doi.org/10.1109/JMEMS.2007.896714.

[15] C. Guan, Y. Zhu, An electrothermal microactuator with z-shaped beams, Journal of Micromechanics and Microengineering 20 (2010) 085014, http://dx.doi.org/10.1088/0960-1317/20/8/085014.

[16] M. Inc., 4021 Stirrup Creek Drive, Durham, NC 27703, USA, http://www.memscap.com.

[17] M. de Boer, D. Luck, W. Ashurst, R. Maboudian, A. Corwin, J. Walraven, J. Redmond, High-performance surface-micromachined inchworm actuator, Journal of Microelectromechanical Systems 13 (1) (2004) 63–74, http://dx.doi.org/10.1109/JMEMS.2003.823236.

[18] Memscap Inc, http://www.memscap.com/__data/assets/pdf_file/0012/1731/PolyMUMPs.faq.v2.pdf.

[19] J. Zárate, K. Ogando, N. La Forgia, H. Pastoriza, Novel uncooled infrared detector, unpublished, 2012.

[20] Coventor Inc., 4000 Centregreen Way, Cary, NC 27513, USA, http://www.coventor.com.

[21] O. Ozsun, B.E. Alaca, A.D. Yalcinkaya, M. Yilmaz, M. Zervas, Y. Leblebici, On heat transfer at microscale with implications for microactuator design, Journal of Micromechanics and Microengineering 19 (4) (2009) 045020, http://dx.doi.org/10.1088/0960-1317/19/4/045020.

[22] A. Atre, Analysis of out-of-plane thermal microactuators, Journal of Micromechanics and Microengineering 16 (2) (2006) 205, http://dx.doi.org/10.1088/0960-1317/16/2/003.